Biomedical Signal Processing and Control 43 (2018) 250–264

Contents lists available at ScienceDirect

Biomedical Signal Processing and Control

journal homepage: www.elsevier.com/locate/bspc

Copula as a dynamic measure of cardiovascular signal interactions

Sladjana Jovanovic[a,*], Tamara Skoric[b], Olivera Sarenac[c], Sanja Milutinovic-Smiljanic[d], Nina Japundzic-Zigon[c], Dragana Bajic[b]

[a] Telecom Serbia, Network and Services Planning and Development Function, Bulevar umetnosti 16a, 11070 Novi Beograd, Serbia
[b] University of Novi Sad, Faculty of Technical Sciences, Center of Excellence for Vibrations, Acoustics and Biomedical Signals CEVAS, Trg Dositeja Obradovica 6, 21000 Novi Sad, Serbia
[c] University of Belgrade, School of Medicine, Laboratory for Cardiovascular Pharmacology, Dr Subotica 1, 11000 Belgrade, Serbia
[d] University of Belgrade, Faculty of Dental Medicine, Dr Subotića 8, 11000 Belgrade, Serbia

ARTICLE INFO

Article history:
Received 28 February 2017
Received in revised form 17 January 2018
Accepted 17 March 2018
Available online 31 March 2018

Keywords:
Copula
Systolic blood pressure
Pulse interval
Pharmacological blockade
Dynamic multivariate dependency
Time lag

ABSTRACT

Objectives: Copula is a tool for measuring linear and non-linear interactions between two or more time series. The aim of this paper is to prove that a copula approach can accurately capture and visualize the spatial and temporal fluctuations in dependency structures of cardiovascular signals, and to outline the application possibilities.
Methods: The method for measuring the level of interaction between systolic blood pressure and the corresponding pulse interval is validated statistically and pharmacologically. The time series are recorded from the freely moving male Wistar rats equipped with radio-telemetry device for blood pressure recording, before and after administration of autonomic blockers scopolamine, atenolol, prazosin and hexamethonium. Implicit (Gaussian and t) and explicit (Clayton, Frank and Gumbel) copulas were calculated and compared to the conventional bivariate methods (Kendal, Pearson, Spearman and classical correlation). Further statistical validation was done using artificially generated surrogate data. A window sliding procedure for dynamic monitoring the signals' coupling strength is implemented.
Results: Under the baseline physiological conditions, SBP-PI dependency is significant for time lags 0 s–4 s. Hexamethonium completely abolished the dependency, scopolamine abolished it for time lags 0 s–2 s, atenolol first slightly increased, than for lags greater than 2 s decreased the dependency and prazosin had no effect. Isospectral and isodistributional surrogate data tests confirm that copulas successfully notify the absence of dependency as well.
Conclusion: Copula approach accurately captures the temporal fluctuations in dependency structures of SBP and PI, simultaneously enabling a visualization of dependency levels within the particular signal zones. An analysis showed that copulas are more sensitive than the conventional statistical measures, with Frank copula exhibiting the best characterization of SBP and PI dependency.

1. Introduction

Ever since the first notion that heart pressure changes are followed by changes in cardiac cycle length (1859, [1]), interactions and control mechanisms of cardiovascular signals have permanently resided in the focus of research attention. Interaction alterations could point to cardiac autonomic dysfunctions as a consequence of various pathological conditions [2,3].

The main short-term regulation mechanism of blood pressure, baroreflex (BRR), has been subject of numerous clinical researches, scientific studies and practical applications. Traditional methods are focused on the assessment of baroreflex sensitivity (BRS) defined as a ratio of changes in pulse interval (PI) per unit change in blood pressure (BP) [4], with the comprehensive reviews in [4–6]. The time-domain cross-correlation method (xBRS) [7] additionally introduces a sliding window and cross-correlation for assessing the time delay (lag) of PI in respect to SBP for which the signal correlation is at its maximum, shown to be an important clinical marker [3,8].

The nonlinear nature of cardiovascular signal dependency, especially in cases of baroreflex impairment, was also pointed out [3,9]. As a complement to the traditional methods, the approaches based on nonlinear dynamics (NLD) were developed. While tradi-

* Corresponding author.
E-mail addresses: sladjanajo@telekom.rs (S. Jovanovic), ceranic@uns.ac.rs (T. Skoric), osarenac@med.bg.ac.rs (O. Sarenac), sanja.milutinovic@stomf.bg.ac.rs (S. Milutinovic-Smiljanic), nzigon@med.bg.ac.rs (N. Japundzic-Zigon), draganab@uns.ac.rs (D. Bajic).

https://doi.org/10.1016/j.bspc.2018.03.007

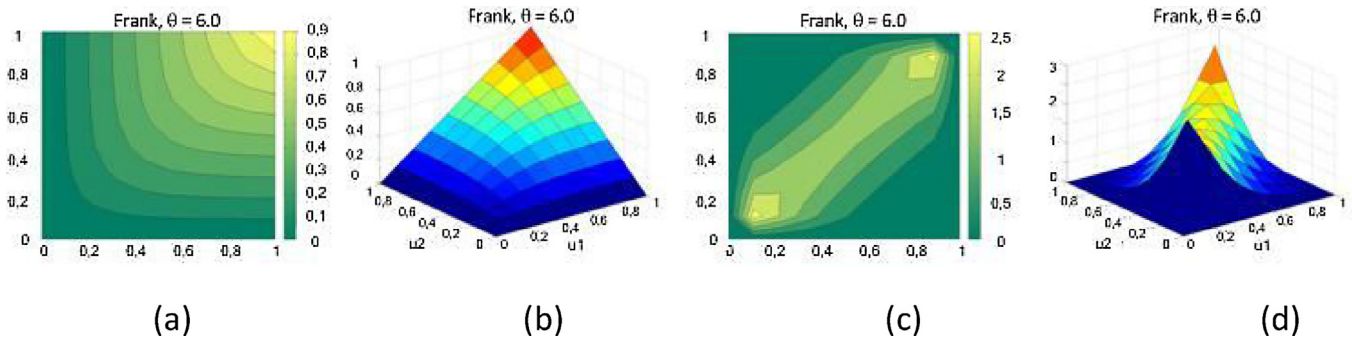

Fig. 1. An example of a bivariate (N = 2) Frank copula with parameter θ=6.0. From left to right, (a) Copula (distribution function); (b) 3D presentation of the same copula; (c) Copula density function; yellow parts point out the regions of increased dependency. (d) 3D presentation of the same density. (For interpretation of the references to colour in this figure legend, the reader is referred to the web version of this article.)

tional methods operate around the set point (linear portion) of the sigmoidal baroreceptor curve [10], NLD methods consider its non-linear shape. These methods could be classified [11] as methods based on a fractal measures, entropy measures, symbolic dynamics measures and Poincareí plot representation [12–15]. Their potential is confirmed by clinical studies [3,16]. Relevant parameters of the methods are highly differing and they require long stationary signals.

This study investigates a copula approach for cardiovascular time series dependency quantification. The approach allows a dynamic presentation, but also a visualization of the signal dependency structure.

A copula is a mathematical concept that decomposes a multivariate distribution function into univariate marginals and into a function that quantifies their statistical dependency. Copula was introduced by Abe Sklar [17] and a great variety of copula functions gives a possibility to model different dependency structures and to measure nonlinear dependencies. It is used in scientific fields that require multivariate applications- e.g. for finance, climate researches, hydrogeology, biomedicine [18–20]. The possibility of applying a copula for cardiovascular signals was pointed out in [21]. In this research, we combine the benefits of the copula to reflect the real signal dependency structure (linear or non-linear) and sliding window applied in the xBRS method [7].

The aim of this contribution is fourfold: a) to prove that the copula approach can accurately capture the dynamic (temporal) fluctuations in SBP and PI dependency, b) to explore the possibility of the copula to analyze dependency structure of joint distribution c) to select a copula family that is adjusted the best to the cardiovascular signals and d) to prove that the evaluated measure is indeed an outcome of autonomic cardiovascular control and not a consequence of some random occurrence.

The paper is organized as follows: the next section gives a brief description of copula as a mathematical concept, followed by a description of a pharmacological experimental protocol. It also includes a block-diagram of the complete procedure. Within the third section different families of copula are compared. Comparison is based on empirical and fitted copula function, and on empirical and artificial data obtained by copula generators. Sensitivity of the system was tested not only for copula methods, but for the other conventional correlation methods too. The assumption that the changes in level of SBP-PI interaction at the different time lags are due to the physiological disturbance is tested by opening the loop of the feedback control mechanisms, thus altering the SBP-PI relationship. It was done by means of the pharmacological blockade using scopolamine, atenolol, prazosin and hexamethonium and also by the artificial independent randomization of SBP and PI signal samples (surrogate data control study). The concluding remarks are given within the last section.

2. Materials and experimental methods

2.1. Copula approach

The basic aim of this study is to implement a copula as a measure of dependency between two or more signals. It also shows that copulas offer other possibilities such as: (1) to describe joint behavior of variables and visualize their dependency structure separated from marginal distributions, via estimated copula density; (2) to capture both linear and non-linear co-dependency of the variables, (3) to find a copula family that represents the dependency structure of the observed signals in the best way [22–24].

The copula theory states that any multivariate (N-variate) distribution can be described by its N independent univariate distributions and its copula [17]. For a set of N variables X_i, with continuous cumulative distribution functions F_i, $i = 1, \ldots, N$, and a joint distribution $H(X_1, \ldots, X_N)$, a new set of N uniformly distributed random variables $(U_1, \ldots U_N) = (F_1(X_1), \ldots, F_N(X_N))$ can be created by applying the probability integral transformation [25]. The inside information of $(X_1, \ldots X_N) = \left(F_1^{-1}(U_1), \ldots, F_N^{-1}(U_N)\right)$ the marginal distributions can be retrieved by the inverse transformation

Copula is a cumulative multivariate distribution function with marginals uniformly distributed on $[0,1]^N$. The relationship between the multivariate joint distribution $H(X_1, \ldots, X_N)$ and the corresponding copula $C(U_1, \ldots, U_N)$is defined by Sklar's theorem [24] as:

$$H(X_1, \ldots, X_N) = C(F_1(X_1), \ldots, F_N(X_N)), \quad (1)$$

and, vice versa:

$$C(U_1, \ldots U_N) = H\left(F_1^{-1}(U_1), \ldots, F_N^{-1}(U_N)\right). \quad (2)$$

For copula visualization, it is more appropriate to use copula density that can be derived as:

$$c(U) : \frac{\partial^N C(U_1, \cdots, U_N)}{\partial U_1 \cdots \partial U_N} \quad (3)$$

Copula density shows a probability that a set of uniform variables $U_i, i = 1, \ldots, N$ would be located within a particular region of $[0,1]^N$ space. This probability corresponds to the level of dependency of variables within this region. An example of a bivariate copula and its density is shown in Fig. 1.

Numerous copula families exist, and it is a challenge to find a copula family that reflects the dependency of the observed signals in the best way. In this study five different copula families were tested to find the one that is a proper choice for cardiovascular signals.

Gaussian copula $C^{(g)}(U)$and t copula $C^{(t)}(U)$ represent a dependency structure implicit in elliptical multivariate normal and

Student t distributions respectively. For a standardized multivariate normal distribution Φ_ρ, the multivariate Gaussian copula [24] is defined as:

$$C^{(g)}(U_1, \cdots, U_N; \rho) = \Phi_\rho\left(\Phi^{-1}(U_1), \cdots, \Phi^{-1}(U_N)\right), \quad (4)$$

For a standardized multivariate Student's distribution $T_{\rho,\nu}$ with ν degrees of freedom, the multivariate t copula is defined as:

$$C^{(t)}(U_1, \cdots, U_N; \rho, \nu) = T_{\rho,\nu}\left(t_\nu^{-1}(U_1), \cdots, t_\nu^{-N}(U_N)\right). \quad (5)$$

For both copulas, the correlation matrix $\boldsymbol{\rho}$ is symmetric and positive definite with values 1 along the main diagonal and with values between −1 and 1 elsewhere. $\Phi^{-1}$and t_ν^{-1} are inverses of the univariate normal and Student t distributions.

Archimedean copulas are subset of wide class of explicit copulas [24,26]. If Archimedean generator is defined as a continuous, strictly decreasing convex function with a positive second derivative, $\Phi : [0, 1] :\rightarrow [0, \infty]$, where is $\Phi(0) = 1$and $\lim_{t\rightarrow\infty}\Phi(t) = 0$, then Archimedean copulas are defined as:

$$C(U) = \Phi\left(\Phi^{-1}(U_1) + \cdots + \Phi^{-1}(U_N)\right), \quad (6)$$

for $U \in [0, 1]^N$. For this study, Clayton copula $C^{(C)}(U)$, Frank copula $C^{(F)}(U)$ and Gumbel copula $C^{(G)}(U)$ were chosen, expressed as [24]:

$$C^{(C)}(U_1, \ldots, U_N) = max\left\{\left(\sum_{i=1}^{N} U_i^{-\theta} - N + 1\right)^{-1/\theta}, 0\right\}, \theta\varepsilon[-1, \infty)/\{0\}, \quad (7)$$

$$C^{(F)}(U_1, \ldots, U_N) = -\theta^{-1} \cdot \log\left[1 + \frac{\prod_{i=1}^{N}\left(e^{-\theta \cdot U_i} - 1\right)}{\left(e^{-\theta} - 1\right)^{N-1}}\right], \theta\varepsilon[-\infty, \infty)/\{0\}, \quad (8)$$

$$C^{(G)}(U_1, \ldots, U_N) = exp\left[-\left(\sum_{i=1}^{N}(-\log(U_i))^{\theta}\right)^{1/\theta}\right], \theta\varepsilon[1, \infty). \quad (9)$$

The copula parameter $\boldsymbol{\theta}$ reflects the level of dependency between the variables and it can be extracted from the set of original signals. The marginal distribution functions of the original signals are first transformed into uniform distribution via the probability integral transform, preserving the link between the simultaneously recorded variables. Then, the N-dimensional empirical distribution function is estimated from the transformed signals, thus creating an empirical copula. The empirical copula is compared to a range of theoretical copulas to find the closest one in a maximum likelihood sense. The parameter $\boldsymbol{\theta}$ of the closest copula shows the dependency level. This process can be repeated for different copula families, with a goal to find out the family that is the most appropriate for the particular type of signals, according to the goodness of fit tests.

Copulas provide a simple method to study, measure and visualize the dependency between the random variables [27]. As a joint distribution function of marginals that are uniform, it shows the probability of concordance and discordance of the observed variables [24]. In a copula world, measures of dependence can be regarded as non-parametric rank correlation coefficients coupled with coefficients of tail dependency. A link between parameters of copula and rank correlation coefficients can be found in literature [27], but the tail dependency characterizes dependency of extreme values of variables. Jointly, they allow copula to capture both linear and non-linear co-dependency.

Linear correlation coefficients cannot be regarded as copula-based measures of dependence. They are suitable for elliptical joint distributions and, even then, there are some heavy tailed distributions where linear correlation is not applicable. If conventional correlation measures were applied outside the class of elliptical distributions and linear relationships, a possibility of pitfalls and erroneous results could have occurred [27,28].

For the sake of comparison, the dependency measures assessed by the copula parameter are compared to the results of the linear Pearson's product-moment correlation, linear cross-correlation applied in xBRS [7], Kendall's rank correlation and Spearman's rank correlations, as they are related to the copula parameter [27]. Pearson's product-moment correlation measures linear relationship between variables. Cross-correlation measures correlation between sequences that slide over each other. Resulting set of cross-correlation coefficients is twice longer than the original set. Kendall's correlation reflects the number of concordances and discordances in time series, regardless of their degree. Spearman's correlation measures the correlation between the ranked data [29].

These coefficients are scalars that provide general information about the level and direction of dependency, but limited information about the dependency shape. Copula parameter is a scalar as well, but the copula itself is a distribution function, allowing an insight into the dependency structure and enabling the visualization of the dependency changes within different copula regions, and in particular within the tail regions.

The bivariate examples of copula families are visualized in Fig. 2. Right panels of Fig. 2 present scatterplots, obtained by generating 1000 U1-U2 pairs of uniform random variables using an appropriate copula generator, and applying an inverse probability integral transform to get normally distributed variables X1–X2. Panels in left and in middle of Fig. 2 show the main characteristics of dependency structure via copula density [30]:

- For Gaussian copula it is centrally symmetric with weak tail dependencies, left and right tail dependencies go to zero at extremes
- For t copula it is centrally symmetric, with a stronger lower left and upper right tails, and weaker upper left and lower right tails
- For Clayton copula it is axially asymmetric, with a strong left tail dependence and weak right tail dependence, right tail dependence to zero at right extreme
- For Frank copula it is centrally symmetric, very weak tail dependencies, left and right tail dependencies go to zero at extremes
- For Gumbel copula it is axially asymmetric, weak left tail dependence, strong right tail dependence, left tail dependence goes to zero at left extreme
- For all copulas orientation from lower left to the upper right corner indicate concordance between variables; a higher concentration around the diagonal indicates a higher level of concordance; in the cases of discordances the structure would be oriented from upper left to the lower right corner

Such different dependency structures characteristic for different copula families provides a way to find out the model that is the most appropriate for the particular type of joint distribution.

2.2. Ethics and experimental protocol

All experimental procedures were conducted in accordance with the European Communities Council directive of 24 November 1986 (86/609/ECC) and the School of Medicine, University of Belgrade Guidelines on Animal Experimentation.

Animals: Experiments were performed on freely moving Wistar outbred rats weighing 330 ± 20 g with food and water ad libitum, in controlled laboratory conditions (22 ± 1 °C, 60 ± 5% relative humidity and 12 h light-dark cycle). The number of animals per group was calculated according to the variability of cardiovascular parameters in the control group of rats using statistical software "Power Sample Size Calc" [http://www.statisticalsolutions.net/pss_calc.php], and it

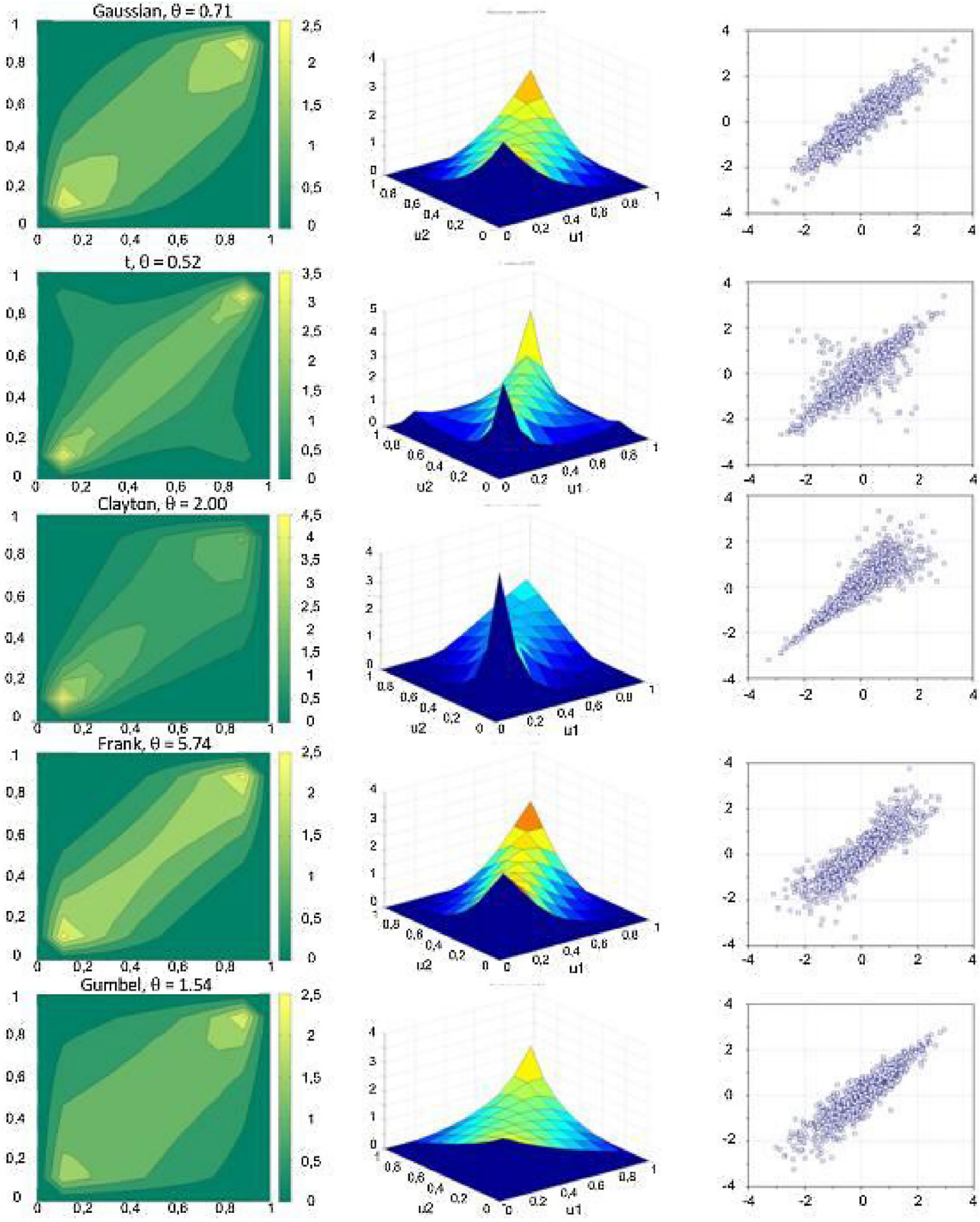

Fig. 2. Examples of five copula families, from top to bottom: Gauss, t, Clayton, Frank, Gumbel. Left panels: 2D presentation of bivariate copula density; Central panels: 3D presentation of the same density; Right panels: scatterplots – 1000 sample pairs generated by a copula generator and transformed by an inverse probability integral transformation. Copula parameter θ shows a level of statistical dependency.

was n = 10. Surgery Under combined ketamine (100 mg/kg, i.m.) and xylazine anesthesia (10 mg/kg, i.m.) radio-telemetric probes (TA11PAC40, DSI, St. Paul, MN, USA) were implanted in abdominal aorta of rats. In the perioperative period rats were treated with gentamicin two days before and on the day of surgery (25 mg/kg, i.m.) to prevent infection. Carprofen (5 mg/kg, s.c.) was applied for pain relief on the day of surgery and for the next two days. Following the seven days recovery period, another quick surgical procedure

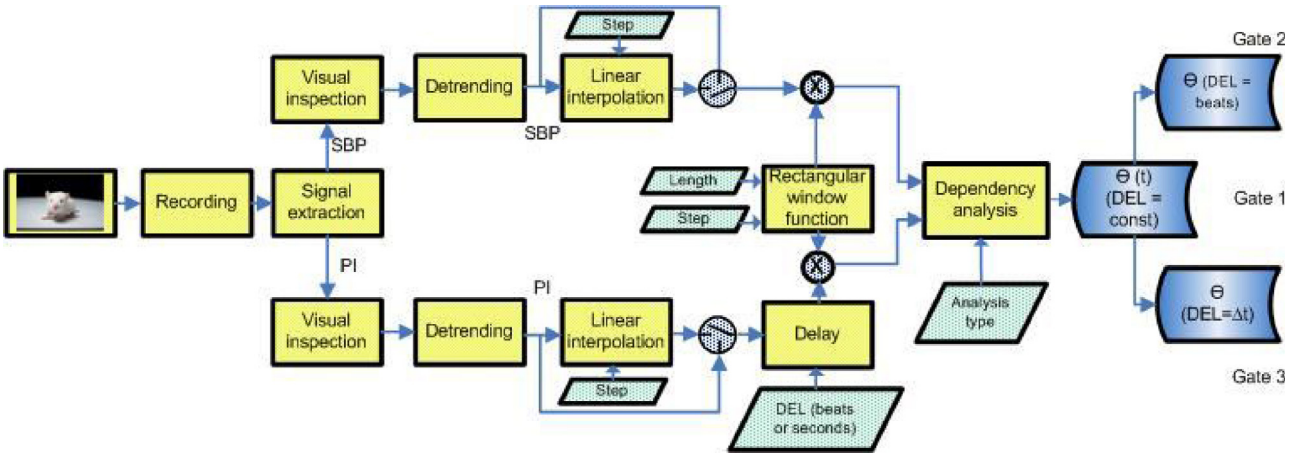

Fig. 3. The block diagram of the signal processing procedure.

was performed to position venous catheter in rat's left jugular veins for drug infusions. Rats were left to recover 48 h during which the catheter was flushed with heparinized saline twice daily to prevent clothing.

Protocol Experiments began at 10 am every day in rats (n = 10) housed individually in Plexiglas cages (25 × 25 × 25) cm under quiet laboratory conditions. After initial baseline recording of arterial blood pressure, rats received saline (0.1 ml/kg, i.v.) to be recorded for 20 min. This was followed by intravenous drug injection: scopolamine (1 mg/kg, i.v.) or atenolol (2 mg/kg, i.v.) or prazosin (1 mg/kg, i.v.) or hexamethonium (20 mg/kg, i.v.) and another 40 min-long recording sessions. The total number of recorded 20 min-long signals was 40, while the number of 40 min-long recordings after the drug administration was 10 for scopolamine, atenolol, prazosin and hexamethonium each.

2.3. Signal acquisition and processing

A block-diagram of the proposed procedure is shown in Fig. 3.

Blood pressure waveforms (BP) were transmitted and digitally recorded using Dataquest A.R.T. 4.0 software (DSI, St. Paul, MN, USA), with sampling frequency fs = 1000 Hz and the corresponding sampling interval ΔT = 1 ms. The systolic blood pressure (SBP) was determined as waveform local maxima. The pulse interval was determined as an interval between the successive moments of maximal gradients $(\Delta(BP)/\Delta T)_{max}$, i.e. the local maximal change (Δ) of blood pressure waveform (BP) per sampling interval. It is an acceptable alternative to R–R interval [31].

SBP and PI signals were visually inspected and artifacts were corrected. A very slow signal component (trend) was eliminated using a high-pass filter designed specifically for biomedical signals [32]. Cut-off frequency was from 0.055 Hz to 0.085 Hz ($0.011/\overline{PI}$[s] [32], $\overline{PI}$ denoting the mean value of the estimated PI series). It is within the very low frequency range in rats, while in humans the frequency ranges are lower [33].

The procedure offers two modes: either to process the original beat-to-beat samples, or to process equidistant samples, obtained by linear interpolation with a step Δt (block "Linear interpolation"). The latter choice enables a true time domain analysis, unbiased by pulse interval changes (i.e. by heart-rate changes). A block "Delay" (in PI branch) controls the delay of pulse interval in respect to SBP, expressed either in number of beats, or, in a case of interpolated equidistant samples, in time units.

The overlapping rectangular window is applied as a multiplicative function. Its role is to mitigate the effects of noise and residual unobserved artifacts by averaging the results over a large number of successive overlapping segments. It also gives the possibility to monitor dynamic temporal changes in the joint distribution function that would otherwise be smoothed out. Finally, it enables an unbiased comparison of long and short records.

Dynamic changes of copula parameter are obtained by a sliding window, as shown in an illustrative example in Fig. 4. Sliding window of length Win = 20 s overlaps the data, starting at the position t = 140 s for SBP, and at the position 140.7 s for PI (i.e. time lag of PI signal in respect to SBP is equal to 0.7 s). The copula parameter is estimated from the data in window. Then windows slides with a step of 5 s, so the new SBP and PI segments start at the positions 145 s and 145.7 s, respectively, enabling the next parameter θ to be compiled.

The illustrative example in Fig. 4 comprise normalized SBP and PI signals that are well aligned with high copula parameter (left panel); a disturbance of PI signal (right panel) causes copula parameter to drop.

The choice of window length Win is an outcome of an engineering compromise. The window should contain a statistically sufficient number of SBP-PI pairs to ensure a reliable estimation of probabilities that correspond to each one of two-dimensional histogram bins that a copula – i.e. a bivariate distribution function – consist of. Only then an empirical copula is a truly reliable estimate. On the other hand, the window must not be too long as the variability in rhythm and nature of the signal segment would be lost thus also deteriorating the signal stationarity. For this reason, the window lengths in this study were 10 < Win < 500 if expressed in seconds, and 100 < Win < 5000 if expressed in number of heart beats. The windows are sliding with a chosen step, usually lengthiness of 2,5 and 5 s or 25 and 50 beats. Such steps are below the window length, so the windows are overlapping.

After the windowing function, one out of nine analytical methods can be chosen – five copulas and four correlations (block "Dependency analysis", Fig. 3). Then three outcomes are possible, denoted as Gate 1, Gate 2 and Gate 3 in Fig. 3.

The output of Gate 1, shown in lower panel of Fig. 5a, yields dynamic temporal fluctuations of dependency measure θ(t, DEL = 0.7 s). Input signals SBP and PI are shown in upper and middle panel respectively. The output of Gate 3, shown in Fig. 5b, presents a two-dimensional dynamic dependency θ(t,DEL), where the second dimension is time delay of PI in respect to SBP signal. It shows the changes of sympathetic and parasympathetic responses, as the length of PI delay reflects its strength – the longer delay, the weaker parasympathetic and stronger sympathetic response [7]. The output of Gate 2 is similar, except for the delay DEL that is not expressed in seconds but in number of beats.

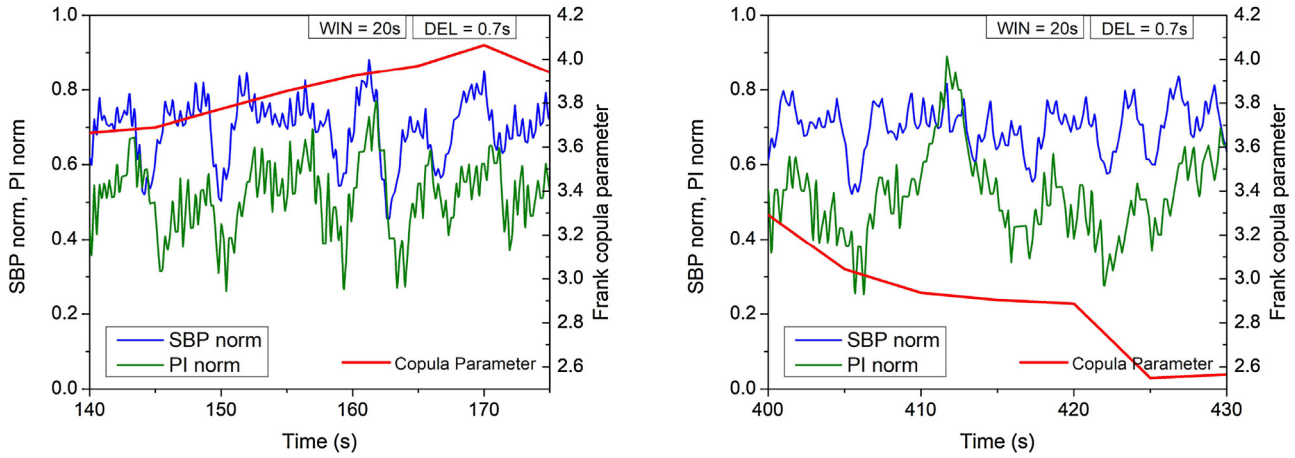

Fig. 4. Changes of the dependency parameter θ(t) for Frank copula (red line); left panel: normalized SBP and PI signals are well aligned; right panel: normalized SBP and PI signals are disturbed and the copula parameter drops. (For interpretation of the references to colour in this figure legend, the reader is referred to the web version of this article.)

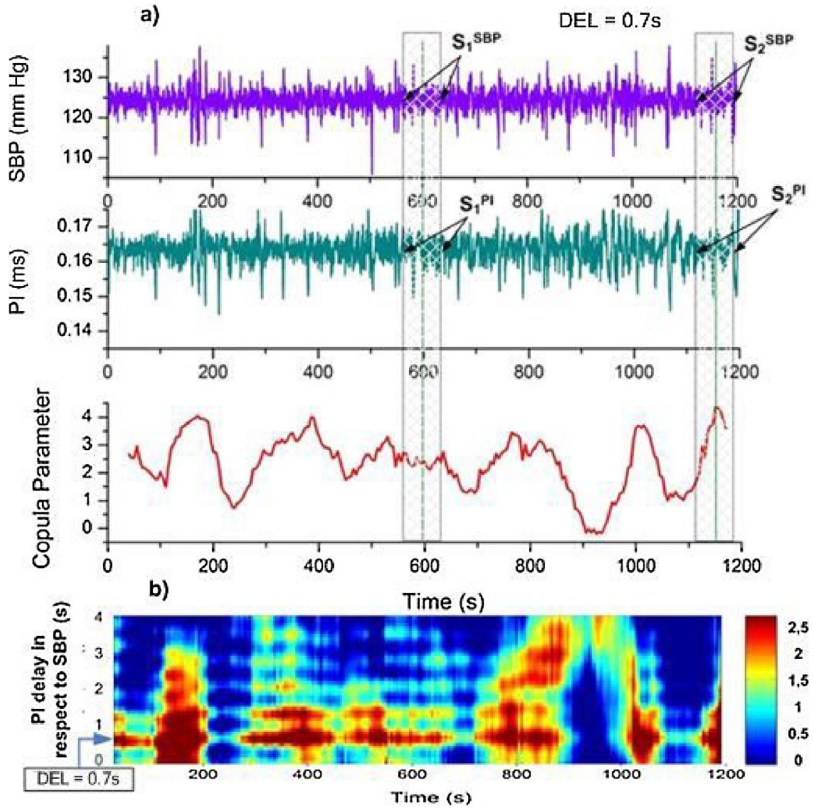

Fig. 5. a) Baseline signals of a rat with marked window sequences S_1 and S_2; upper panel: SBP signal; middle panel: PI signal delayed 0.7 s in respect to SBP; lower panel: Temporal changes of Frank copula parameter for PI signal delayed 0.7 s in respect to SBP (dynamic copula, gate 1 in Fig. 3); b) Dynamic changes of dynamic dependency θ(t,DEL) for different PI delays in respect to SBP; dependency level is marked by color, from blue (lowest) to red (highest); delay 0.7 s from the previous panel is marked by a light blue arrow. (For interpretation of the references to colour in this figure legend, the reader is referred to the web version of this article.)

Fig. 6 presents the dependency parameter averaged over all windows. Dependency is evaluated as a function of delay that is expressed in beats (left panel) and in seconds (middle panel). Panel in right compares Frank copula parameter evaluated for delays both in beats and in seconds. The compliance between the results is evident.

3. Results

3.1. Comparative analysis and copula family choice

For a detailed copula analysis, two SBP-PI signal pairs are observed, shown in shaded windows of Fig. 5a and enlarged in

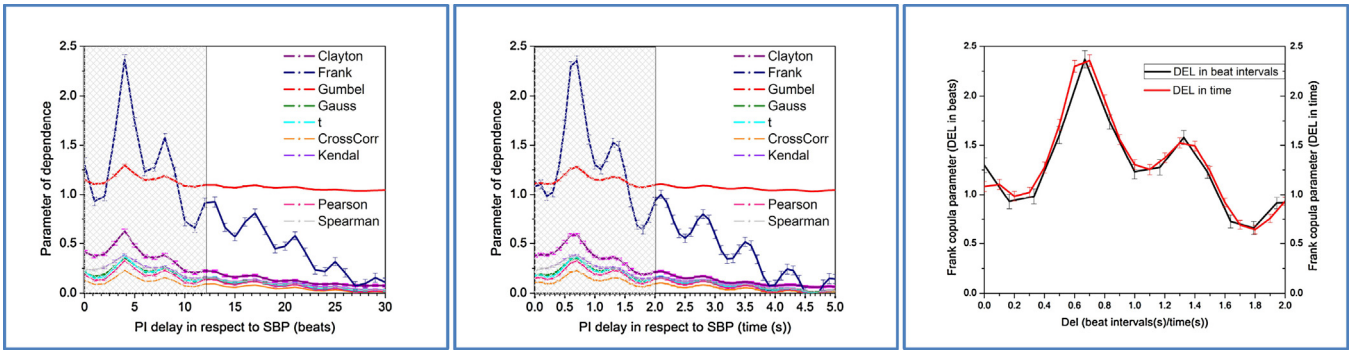

Fig. 6. Dependency parameter of PI response in respect to SBP, evaluated using five copula methods and four conventional (bivariate) methods; left panel: signal on Gate (2); middle panel: signal on Gate (3); right panel: comparison of Frank copula parameters for delay expressed in beats and in seconds.

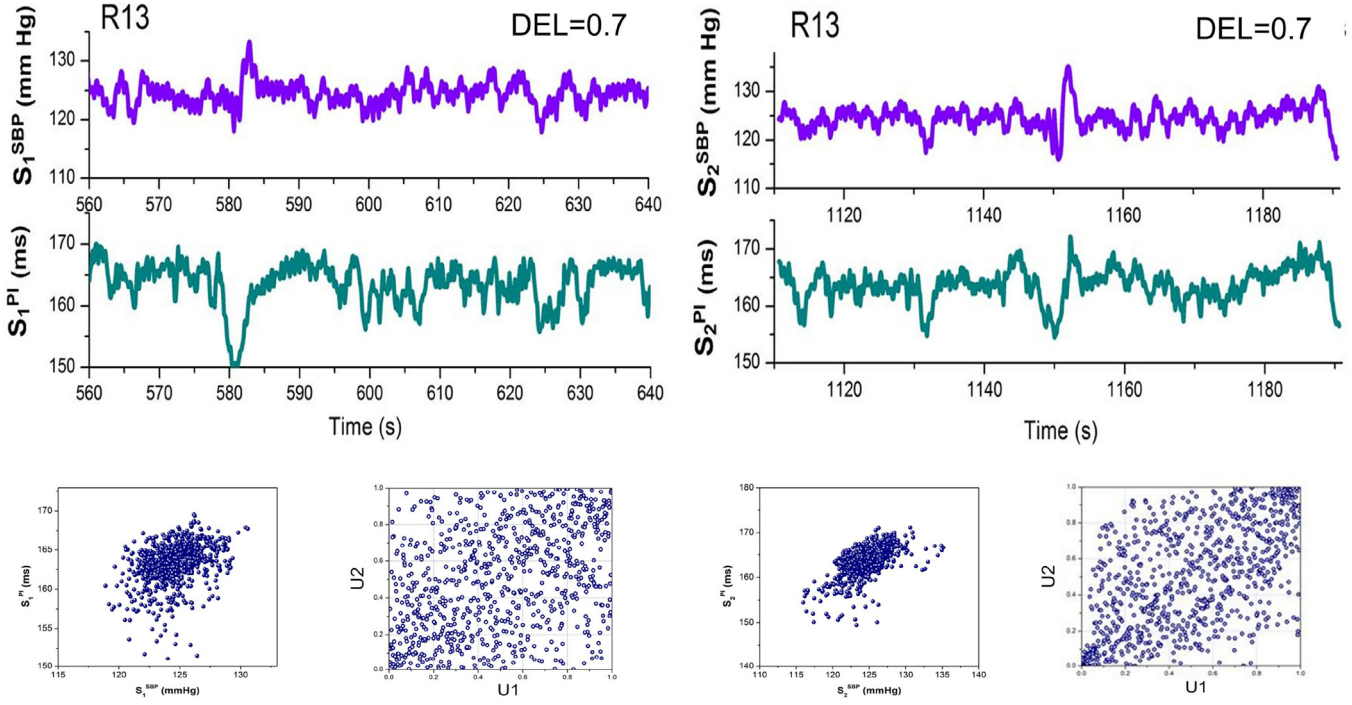

Fig. 7. Enlarged signals from windows in Fig. 5 and the corresponding scatterplots. Upper panels: signals $\boldsymbol{S_1^{SBP}}$ and $\boldsymbol{S_1^{PI}}$ from the first window (left); signals $\boldsymbol{S_2^{SBP}}$ and $\boldsymbol{S_2^{PI}}$ from the second window (right). Lower panels: scatterplots, from left to right, original $\boldsymbol{S_1^{SBP}} - \boldsymbol{S_1^{PI}}$ signals, the corresponding U_1-U_2 signals, original $\boldsymbol{S_2^{SBP}} - \boldsymbol{S_2^{PI}}$ signals, the corresponding U_1-U_2 signals.

Fig. 7. Lower panels of Fig. 7 present the corresponding scatterplots before and after the probability integral transformation. The delay of PI in respect to SBP is chosen to be DEL = 0.7 s, since all nine tested methods exhibited maximal dependency at this particular delay (Fig. 6).

A copula family suitable for cardiovascular signals is selected according to the following criteria: root mean squared error between the estimated and fitted copulas, tail dependency test, artificial and genuine distribution comparison and sensitivity test.

Root-mean-square error (RMSE) is calculated between the empirical copula $C_n(u_1, u_2)$, estimated from n samples of the $\mathbf{X}$–$\mathbf{Y}$ ($\mathbf{S}^{\mathrm{SBP}} - \mathbf{S}^{\mathrm{PI}}$) time series, and its fitted counterpart $C(u_1, u_2)$:

$$RMSE = \sqrt{\frac{1}{n}\sum_{i=1}^{n} (C(U_{1i}, U_{2i}) - C_n(U_{1i}, U_{2i}))^2}, \qquad (10)$$

$$C_n(u_1, u_2) = \frac{1}{n}\sum_{i-1}^{n} \boldsymbol{I}\left\{U_{1i,n} \le u_1, U_{2i,n} \le u_2\right\}, U_{1i,n=}\frac{1}{n}\sum_{j=1}^{n} \boldsymbol{I}\left\{X_j \le X_i\right\}$$

$$, U_{2i,n=}\frac{1}{n}\sum_{j=1}^{n} \boldsymbol{I}\left\{Y_j \le Y_i\right\}.$$

where $\mathbf{I}\{\}$ is an indicator function that is equal to one if the condition in braces is fulfilled [34]. The results are presented in Table 1. The empirical and calculated copulas corresponding to the extreme error values from Table 1 are plotted in Fig. 8.

Tail dependency modeling is an important characteristic of copula. Tails are regions of joint distribution functions corresponding to the extreme marginal values. The important features of tail distribution and dependency are upper and lower tail dependence

Table 1
RMSE·10^{-3} between empirical and fitted copulas.

RMSE between empirical and fitted copula:	Gaussian copula	t copula	Clayton copula	Frank copula	Gumbel copula
for S_1^{SBP} and S_1^{PI}	5.277	5.472	12.747	4.412	8.640
for S_2^{SBP} and S_2^{PI}	5.704	5.593	11.444	5.540	9.529

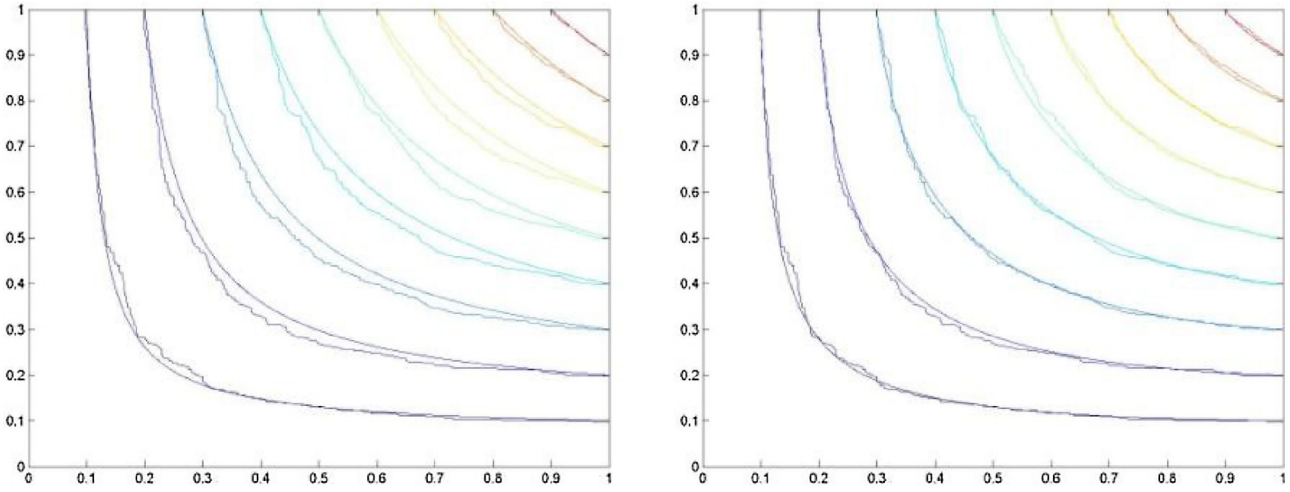

Fig. 8. Empirical copula (distribution function) estimated from $S_1^{SBP} - S_1^{PI}$ signals plotted with its calculated counterpart (smooth lines): left panel, Clayton copula with maximal RMSE from Table 1 (12.747·10^{-3}); right panel: Frank copula with minimal RMSE from Table 1 (4.412·10^{-3}).

Table 2
RMSE·10^{-3} between the tail concentration functions of empirical and fitted copulas.

RMSE between empirical and fitted copula:	Gaussian copula	t copula	Clayton copula	Frank copula	Gumbel copula
$\mathbf{S}_1^{SBP} - \mathbf{S}_1^{PI}$ pair	7.179	8.777	11.444	7.030	9.529
$\mathbf{S}_2^{SBP} - \mathbf{S}_2^{PI}$ pair	9.003	9.791	12.444	9.130	11.292

coefficients λ_u and λ_l (TDC) and tail concentration function $r_c(q)$ (TCF) [35]:

$$\lambda_u := \lim_{q\to 1} P(Y > F_Y^{-1}(q) | X > F_X^{-1}(q)) = \lim_{q\to 1} \frac{1 - 2q + C(q,q)}{1-q}, \quad (11)$$

$$\lambda_l := \lim_{q\to 0} P(Y \le F_Y^{-1}(q) | X \le F_X^{-1}(q)) = \lim_{q\to 0} \frac{C(q,q)}{q}, \lambda_u, \lambda_l, \mathrm{q} \in [0,1] \quad (12)$$

$$r_c(q) = \frac{C(q,q)}{q} \cdot \mathbf{I}\{0 < q \le 0.5\} + \frac{1 - 2q + C(q,q)}{1-q} \cdot \mathbf{I}\{0.5 < q < 1\} \quad (13)$$

The tail concentration function analysis is applied to empirical copula and to all five types of fitted copulas (Fig. 9). Root-mean-square errors between the empirical and fitted TCFs are presented in Table 2.

The goodness of fit (GoF) test shows whether the artificial SBP-PI values generated by copula generator fit to the original SBP-PI values. For this test, U_1–U_2 values with uniform distribution are generated and converted to the artificial SBP – PI samples applying the inverse of probability integral transform. GoF values are presented in Table 3, averaged over 50 sequences per particular copula.

Table 3
GoF test based on normalized RMSE between the original signal and 50 artificially generated signals with copula distribution.

	$\mathbf{S}_1^{SBP}$	$\mathbf{S}_1^{PI}$	$\mathbf{S}_2^{SBP}$	$\mathbf{S}_2^{PI}$
Gauss	1.40 ± 0.04	1.38 ± 0.04	1.41 ± 0.03	1.37 ± 0.04
t	1.38 ± 0.03	1.36 ± 0.02	1.37 ± 0.04	1.35 ± 0.03
Clayton	1.41 ± 0.06	1.39 ± 0.04	1.42 ± 0.03	1.39 ± 0.04
Frank	1.36 ± 0.04	1.37 ± 0.03	1.37 ± 0.02	1.36 ± 0.05
Gumbel	1.41 ± 0.03	1.40 ± 0.04	1.42 ± 0.04	1.41 ± 0.05

Results are presented as mean ± s.e.m (standard error of mean).

As an illustrative example, for each one of the copula types, a copula parameter θ is estimated from both $\mathbf{S}_1^{SBP} - \mathbf{S}_1^{PI}$ and $\mathbf{S}_2^{SBP} - \mathbf{S}_2^{PI}$ signal pairs. The artificial U_1 and U_2 are generated for particular θ values. Then SBP and PI values are calculated by applying an inverse probability integral transform. The scatterplots are presented in Fig. 10, allowing a comparison to the scatterplots of the real signals (lower panels of Fig. 7).

The influence of window length is shown in Fig. 11. The dependency parameter θ for different delays of PI in respect to SBP is calculated for window sizes of 10 s, 30 s, 50 s, 100 s, 250 s and 500 s and plotted for five copula types and four correlation methods. The change of parameter θ in respect to window length is shown in Table 4 at DEL = 0.7 s.

For the next test, the SBP and PI signals were separated into the sequences of duration 10 s, 30 s, 50 s, 100 s, 250 s and 500 s. For each one of the obtained SBP-PI sequence pairs, a copula parameter was estimated and submitted to the copula generator. Then an inverse of the probability integral transform is applied to thus obtained uniformly distributed random sequences. The resulting artificial signals comprised all of the generated sequences of the same length. To test whether the artificial and original signals are from the same distribution, the nonparametric Kolmogorov-Smirnov test is applied. The results are shown in Table 5 and 6 respectively.

Sensitivity at the adjacent time lags shows a significance of signal dependency change along the axis of PI delay in respect SBP. A null hypothesis is that the changes at the neighboring time lags (expressed in beats or in seconds) are not statistically significant. A probability that null hypothesis is accepted is obtained by the ANOVA-F test and it is shown in Fig. 12.

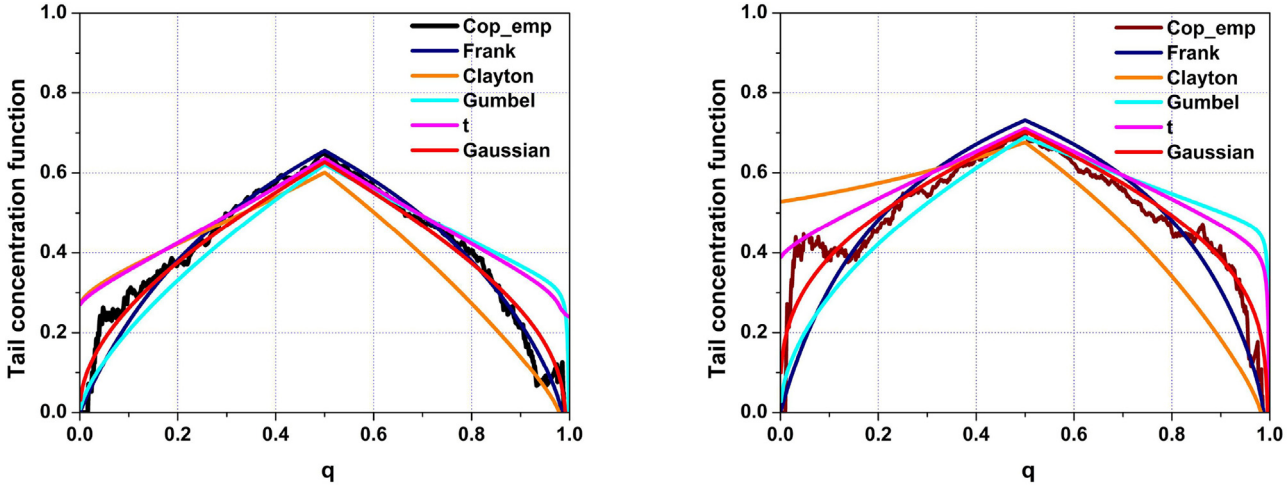

Fig. 9. Tail concentration function of empirical and fitted copulas; left panel: $S_1^{SBP} - S_1^{PI}$ signals; right panel: $S_2^{SBP} - S_2^{PI}$ signals.

Table 4
Maximal change of dependency parameter in respect to window length.

	Extreme values of parameter θ for different window lengths (DEL = 0.7s)								
	Gauss	t	Clayton	Frank	Gumbel	Kendal	Pears.	Spear.	CrossCorr
max θ	0.384	0.428	0.799	2.972	1.477	0.263	0.392	0.368	0.386
min θ	0.346	0.351	0.555	2.312	1.257	0.219	0.371	0.315	0.360
Absolute change θ	0.038	0.077	0.244	0.659	0.220	0.044	0.021	0.053	0.026
Relative change [%]	10.7	20.5	38.7	27.3	16.7	18.9	5.4	16.0	6.9

Table 5
p - value for a two-sided Kolmogorov-Smirnov test at the default 5% significance level for original and artificially generated SBP data series.

	p - value for SBP data series					
	Window length					
	10s	30s	50s	100s	250s	500s
Clayton	0.442	0.522	0.640	0.669	0.619	0.590
Frank	0.529	0.755	0.761	0.787	0.720	0.790
Gumbel	0.480	0.572	0.561	0.598	0.423	0.518
Gauss	0.521	0.606	0.660	0.765	0.729	0.696
t	0.469	0.581	0.638	0.660	0.646	0.629

Table 6
p - value of a two-sided Kolmogorov-Smirnov test at the default 5% significance level for original and artificially generated PI data series.

	p - value for PI data series					
	Window length					
	10s	30s	50s	100s	250s	500s
Clayton	0.345	0.509	0.444	0.532	0.507	0.589
Frank	0.486	0.726	0.652	0.662	0.738	0.725
Gumbel	0.404	0.528	0.511	0.449	0.589	0.432
Gauss	0.476	0.634	0.601	0.689	0.645	0.630
t	0.247	0.529	0.569	0.631	0.634	0.628

Table 7
RMSE·10^3 between empirical and fitted copulas.

	Baseline	Scopolamine	Atenolol	Prazosin	Hexamethonium	Surrogate
Gauss	7.9 ± 1.7	8.3 ± 1.8	10.1 ± 1.9	10.7 ± 4.3	6.6 ± 1.4	6.1 ± 0.9
t	6.6 ± 1.2	8.0 ± 2.1	9.6 ± 1.9	9.6 ± 4.2	6.5 ± 1.7	6.1 ± 0.9
Clayton	11.4 ± 2.1	18.5 ± 11.6	10.5 ± 3.3	12.43 ± 5.3	9.9 ± 2.4	6.0 ± 0.8
Frank	6.1 ± 1.4	8.2 ± 2.2	9.2 ± 2.0	9.8 ± 4.8	6.5 ± 1.8	6.1 ± 0.8
Gumbel	10.2 ± 2.3	19.0 ± 10.1	11.7 ± 3.5	11.6 ± 4.1	8.5 ± 2.7	6.3 ± 0.7
Empirical copula density	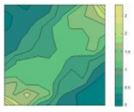	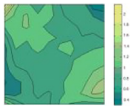	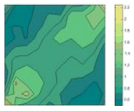	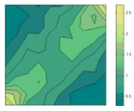	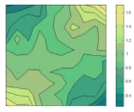	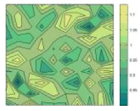

Results are presented as mean ± s.e.m and multiplied by 1000.

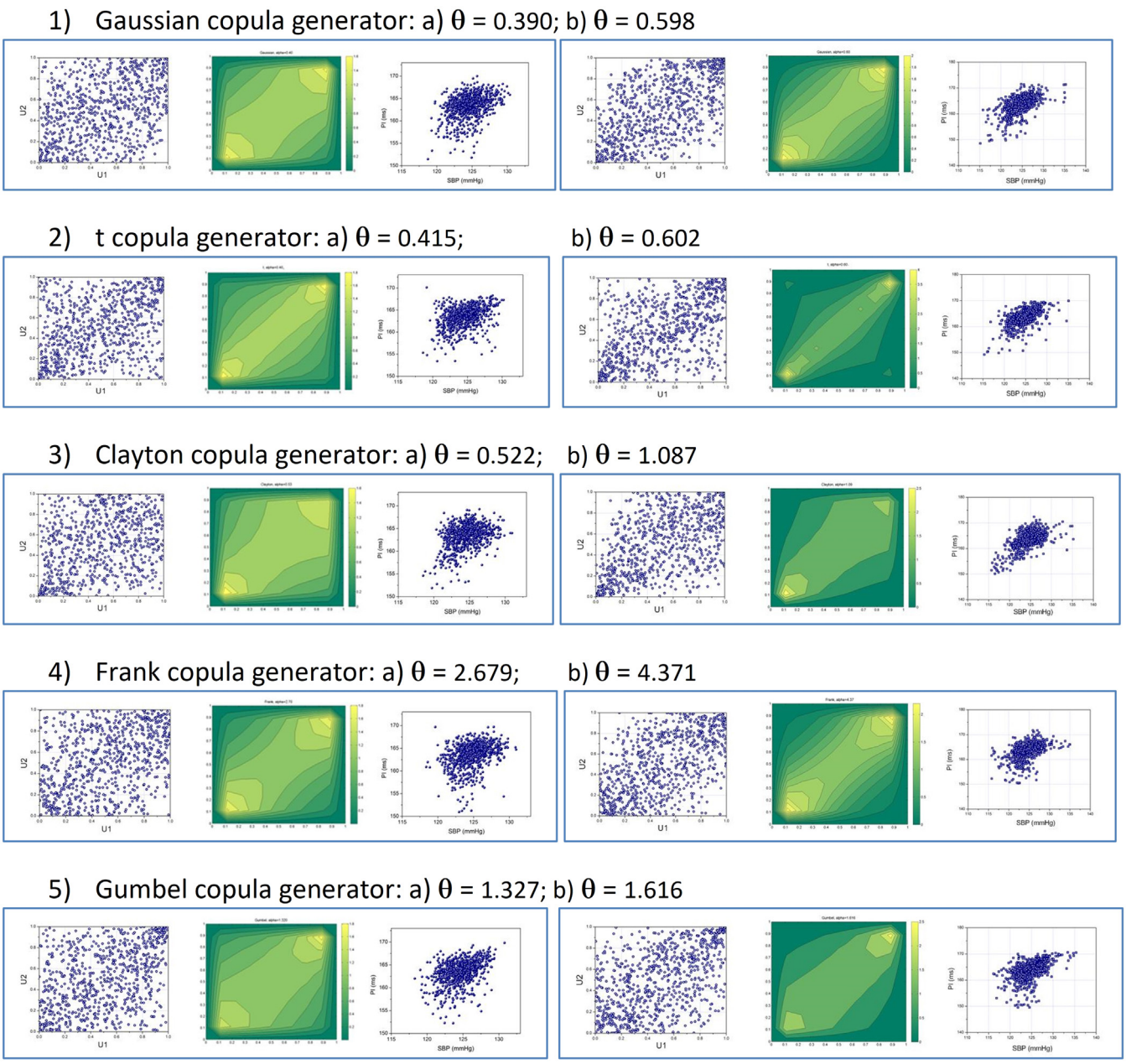

Fig. 10. Artificially generated signals for five copula types. From left to right, U_1-U_2 scatterplot, calculated copula density, artificial $S_1^{SBP} - S_1^{PI}$ scatterplot; θ corresponds to real $S_1^{SBP} - S_1^{PI}$ signals; same plot types are repeated for θ of real $S_2^{SBP} - S_2^{PI}$ signals.

The final test considered the ability to model the dependency in different conditions caused by drug administration. A root mean squared error between the empirical copula and each one out of five types of fitted copula was calculated. The results are shown in Table 7, including the surrogate data copula. For the sake of illustrative comparison, the empirical copula densities are shown within the last table row.

3.2. Pharmacological validation and surrogate data tests

The pharmacological validation is performed to prove that a change in coupling strength between SBP and PI signals is indeed due to the changes in autonomic cardiovascular control. Four types of pharmacological blockades are applied. The analyses were performed using Frank copula for linearly interpolated SBP and PI signals with equidistant samples $\Delta t = 100$ ms, window size 10 s and window overlapping step 2.5 s. Each one of SBP-PI signal pairs is accompanied with a control set of 50 iso-distributional surrogate signal pairs (signals where the temporal relationship is destroyed by random permutation of original signal samples) [36], and 50 iso-spectral surrogate signal pairs where the signals were Fourier transformed, the phases randomized, and the signal submitted to the inverse Fourier transform [37,38]. In the latter case signals preserve the original power spectral density, and, according to the Wiener-Khinchin theorem, the autocorrelation function (provided that the signals are stationary at least in a wide sense) [38]. Two types of phase randomization were applied, the phases substituted by an independent and identically distributed white noise according to [37], and the original phases in randomized order, as described in [39].

Scopolamine is a selective muscarinic receptor antagonist, and as such it blocked the effects of the vagus on the heart

Table 8
Systolic blood pressure and pulse interval of signals at baseline condition and after drug administration.

	Baseline		Pharmacological Blockade	
	SBP [mmHg]	PI [ms]	SBP [mmHg]	PI [ms]
Scopolamine	117.78 ± 2.92	169.41 ± 5.67	127.26 ± 3.38**	143.95 ± 4.33**
Atenolol	120.91 ± 2.39	166.64 ± 6.32	114.77 ± 2.68	189.01 ± 1.58**
Prazosin	118.52 ± 2.47	166.95 ± 7.69	110.90 ± 3.08*	147.22 ± 3.89**
Hexamethonium	118.35 ± 3.18	168.50 ± 8.6	100.19 ± 4.09*	146.56 ± 10.62

The results are presented as mean ± s.e.m. The statistical significance of Blockade versus Baseline was assessed using repeated measures ANOVA test at levels $p < 0.05$ (*) and $p < 0.01$ (**).

Table 9
Frank copula parameter θ at DEL = 0.7 and at DEL = 2.5s, at baseline condition and after drug administration; the results are presented as mean ± s.e.m.

	Delay = 0.7s		Delay = 2.5s	
	Baseline	Blockade	Baseline	Blockade
Scopolamine	2.078 ± 0.118	−0.680 ± 0.212***	0.678 ± 0.109	0.704 ± 0.067
Atenolol	1.539 ± 0.109	2.123 ± 0.175**	1.064 ± 0.090	1.012 ± 0.177
Prazosin	2.049 ± 0.102	1.930 ± 0.073	1.077 ± 0.105	1.474 ± 0.072***
Hexamethonium	2.110 ± 0.142	0.300 ± 0.069***	0.771 ± 0.109	0.178 ± 0.048***

The statistical significance of Blockade versus Baseline was assessed using repeated measures ANOVA test at levels $p < 0.01$(**) and $p < 0.001$(***).

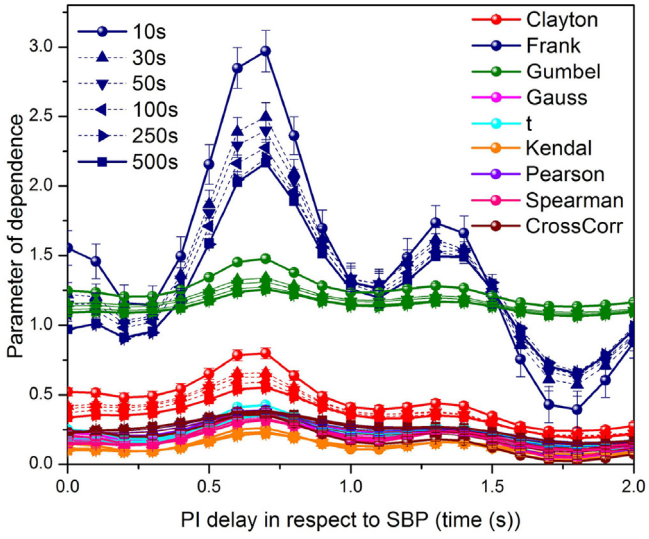

Fig. 11. Dependency parameter for different window lengths.

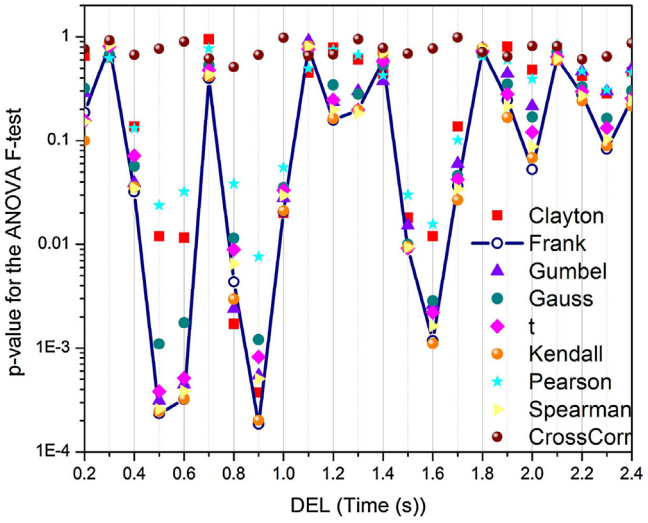

Fig. 12. Statistical significance of dependency parameter changes in respect to its adjacent values, obtained from SBP and PI signals at baseline conditions.

inducing statistically significant tachycardia followed by an increase of SBP. Atenolol prevented the effect of the sympathicus on the heart by blocking beta adrenergic receptors and thus produced slowing of the heart as denoted in PI lengthening. Prazosin, an alpha adrenergic antagonist and hexamethonium, ganglionic blocker, prevented transmission through efferent branches of the sympathetic nerves innervating resistance arteries and thus decreased SBP that in turn produced reflex tachycardia i.e. PI shortening. These changes are confirmed in Table 8.

The experimental outcomes are presented in Fig. 13 and in Table 9, for Frank copula parameters and cross-correlation coefficients averaged over all animals. The maximal delay time of PI was set to 7 s (left panels). Right panels enable a clearer insight into the dependency changes during the first second of PI delay. The figure also plots cross-correlation as a validated method for defining a time lag for maximum dependence of SBP and PI signals [7]. The mutual relationship of Frank copula parameters and cross-correlation coefficients is expressed via Kendall correlation.

The effects of the vagal nerve are the strongest for delay less than one second [40,41]. The Scopolamine-induced blockade prevents the interaction and during the first second there is no positive PI response (Fig. 13, top panels). Then the dependence gradually recovers, and becomes aligned with the baseline status after the sympathetic nervous system induces its (delayed) interactions. The compliance between Frank copula parameters and cross-correlations coefficients is high, for Baseline series and scopolamine series Kendall's tau is 0.94 and 0.79 respectively.

The counter-monotonic behavior during the first second of PI delay after administering scopolamine is partly due to an increased number of "anti-parallel" sequences, where an increase of SBP is followed by a decrease in PI and vice-versa [42]. The number of sequences of all types (without the minimal length constraint) is shown in Table 10.

After administering atenolol, dependency measure during the first second increases in respect to the baseline values (Fig. 13, second row of panels). After the first second, the dependency decreases with higher rate than in baseline. This is in accordance with the blockade of sympathetic nervous system induced by atenolol [40,41], that should be active after the first second. For Baseline series, Kendall's tau is 0.92, while for atenolol series, Kendall's tau is 0.80.

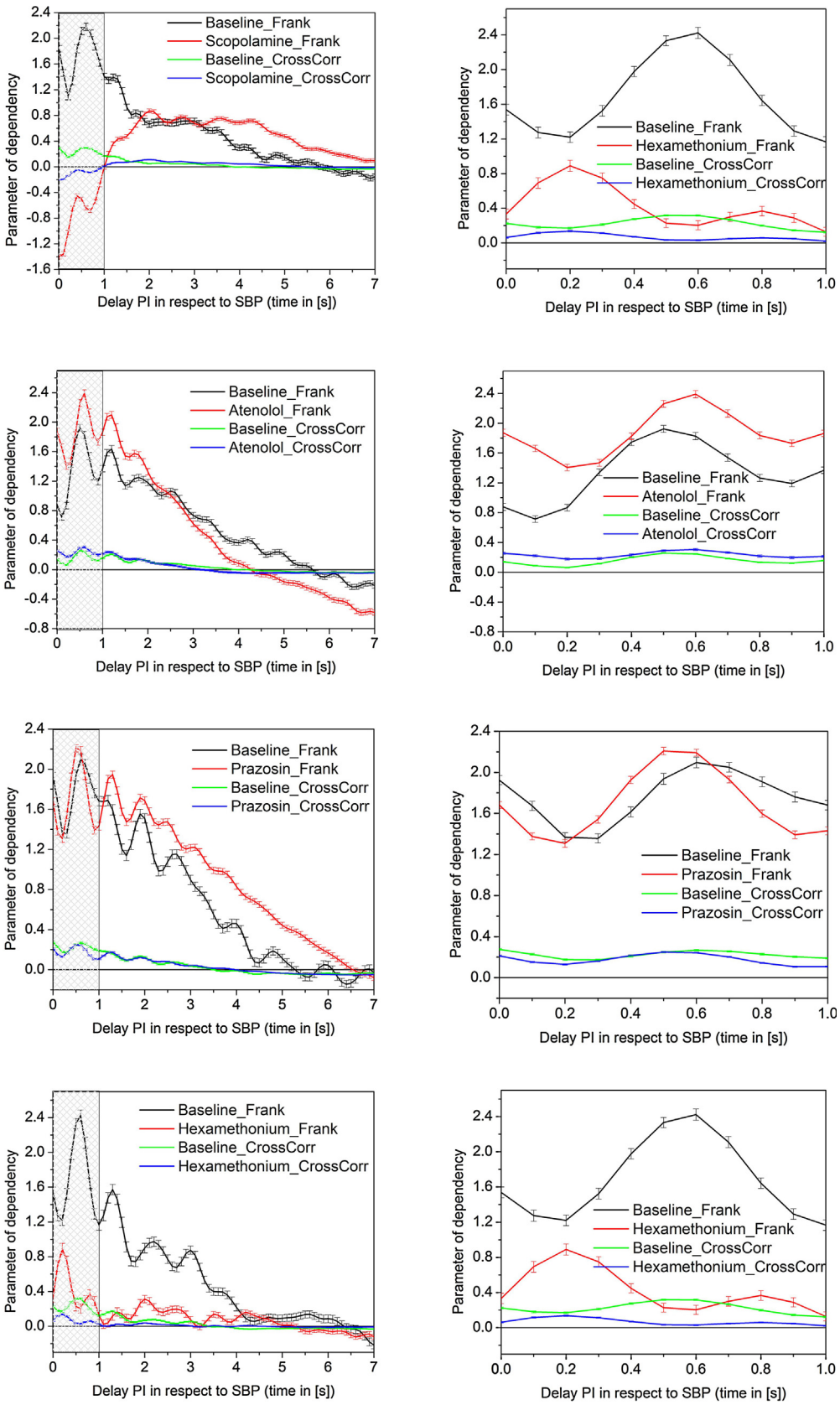

Fig. 13. From top to bottom: Dependency parameter indicating the influence of scopolamine, atenolol, prazosine and hexamethonium; Left panels: the dependence plotted against the PI – SBP delay; Right panels: enlarged shaded detail of PI response in respect to SBP during the first second.

The dependency parameter after administering prazosin is perfectly aligned with the baseline status during the first two seconds (Fig. 13, third row of panels). During the next four seconds the dependency slightly decreases: prazosin dilates arterioles and decreases peripheral resistance by acting on alpha-1 receptors located on arterial vascular smooth muscle. Although prazosin does not influence directly the heart it induced reflex increase of sympathetic outflow to the heart as indicated by increase in HR (Table 8) [43,44]. Kendall's tau as a measure of correlation between Frank copula parameters and cross-correlation coefficients is 0.88 for Baseline signals, and 0.92 for prazosin signals.

Table 9 reveals significant changes in Frank copula parameter at the time lag 0.7 s for scopolamine and hexamethonium ($p < 0.001$) and atenolol ($p < 0.01$) in respect to baseline conditions; the changes are also significant for prazosin and hexamethonium ($p < 0.001$) at the time lag 2.5 s. The changes are in accordance with the known pharmacological effects of the administered drugs, as it would be elaborated in the Discussion.

Results shown in bottom panels of Fig. 13 are in accordance with the effects of hexamethonium that induce a complete sympathetic blockade and partial cardiac parasympathetic blockade [45]. For the time delay suitable for a response of parasympathetic nervous system, the copula parameter after hexamethonium is significantly lower than in baseline. For the time delay suitable for a response of sympathetic nervous system the copula parameter is almost annulled. Kendall's tau is 0.86 for Baseline series, and 0.83 for a hexamethonium series.

The results considering the surrogate data are shown in Fig. 14. Left panel shows copula parameters for original signal and for three types of surrogates. Autocorrelation functions of SBP and PI isodistributional surrogates have no side-lobes and the respective copula parameter is close to zero. Autocorrelation functions of original SBP and PI signals and their isospectral surrogates are identical (right panel), but the phase randomization destroys the cross-sample dependency so copula parameters are again close to zero.

4. Discussion

The analyses performed in Section 3.1 point out that Frank, Gaussian and t copula are the most appropriate ones for BP-PI interactions. This result was not unexpected, as the physiological constraints limit the occurrence of excessive values in biomedical signals, so their probability densities functions are with no emphasized tails. Clayton and Gumbel copulas showed poorer results, as they are fit to distributions with heavy and asymmetric tails. Besides, as it is also verified by cross-correlation, the biomedical signals can exhibit counter-monotonic behavior which Clayton and Gumbel cannot distinguish.

Root mean square errors between the empirical and fitted copulas show that in most cases Frank copula outperforms its Gaussian and t counterparts. Actually, root mean square error are small and mutually similar for all the investigated copula types, showing that in each copula family a representative that resembles an empirical copula can be found. However, minimum of all the minimal errors is obtained with Frank copula (Table 1) that in most cases outperforms its Gaussian and t counterparts. The same result holds for the root mean square error between the tail concentration functions (Table 2).

The goodness-of-fit test is performed for fifty artificially generated signals with particular copula distributions versus empirical copula. The distributions of signals generated by Frank copula generator (joint copula distribution, and distribution of generated SBP and PI signals) are the closest to the distribution of the original SBP and PI signals (Tables 3, 5 and 6).

Effects of window length are shown in Fig. 11. Although the position of maximal and minimal value of parameter θ remains the same along the axis showing PI delay time, the window length influences its value. It is particularly exhibited in Clayton and Frank copula, as their range and sensitivity outperform the other investigated methods.

Increased sensitivity makes a copula vulnerable to parameter changes, including the window length. However, if the window size remains constant during the complete experiment, the relative changes of parameter θ remain unaltered. This conclusion is important for tracking the dynamic changes, as window sliding procedure implies the stationarity of the data inside the window. Additionally, the results of nonparametric Kolmogorov-Smirnov test that compares the distribution of original and artificial signals based on copula generated sequences of a length that correspond to window size showed advantages of Frank, t and Gaussian copula. The lowest level of similarity is evident for the shortest artificial signals, due to the sample size too small to achieve the statistical reliability.

Sensitivity (Fig. 12) is expressed as the probability that hypothesis that no statistically significant changes exist at the adjacent time lags is true. The probabilities for Frank copula lower-bounds the remaining ones (thick line in Fig. 12). Its smallest values correspond to the most significant changes and perfectly match the changes of copula parameter in Fig. 11.

The previous results show that Frank copula slightly outperform the results of its Gaussian and t competitors, but its major advantage is the explicit definition given by Eq. (8). The procedure of finding a theoretical copula that is the closest to the empirical one requires considerably less processing time if an explicit formula can be used.

The pharmacological validation showed that the dependency parameter indeed reflected the cardiovascular system behavior, as shown in Table 9 and Fig. 13: scopolamine inhibited efferent pathway of parasympathetic nervous system and produced a drop of copula parameter in time corresponding to the highest vagal activity (DEL = 0.7 s); atenolol inhibited efferent pathway of sympathetic nervous system and copula parameter starts to drop, becoming significantly lower than in baseline condition after DEL = 2.5 s, corresponding to the activity of sympathetic nervous system. Prazosin did not influence directly baroreflex functionality, but produced an increase of copula parameter at DEL = 2.5, as a secondary drug effect. Hexamethonium inhibited efferent pathways in ganglions of parasympathetic and sympathetic nervous systems, and, accordingly, the drop of copula parameter is obvious in the time periods suitable for activity of both of the branches of autonomic nervous system. In addition to pharmacological validation, Fig. 13 also presents the dependency measured by cross-correlation method [7]. Both copula and cross-correlation captured the same fluctuation of dependency parameter, and the high level of their compliance is quantified by Kendall's correlation test.

The comparison of copula parameter within the first second of PI delay (Fig. 13, right panels) to the empirical copula densities (DEL = 0.7 s) (Table 7, last row) reveals that the dependency structures in baseline, atenolol and prazosin are similar to Frank model: the dependency concentration is close to the diagonal and oriented from lower left to upper right corner, indicating high level of positive concordance between SBP and PI. The dependence structure after hexamethonium reveals similarity both to Frank and to t model (Fig. 2), again indicating concordance, but weak: the dependency is loosely spread along the diagonal, resembling the copula of surrogate data (surrogate density in Table 7), so the parameter θ is low (Fig. 13, bottom right panel). Considering the Scopolamine, the corresponding copula (again similar both to Frank and t model) have different orientation in respect to all the other ones – from the upper left corner to the lower right corner in Table 7. This is in accordance with negative copula parameter θ shown in Fig. 13 and

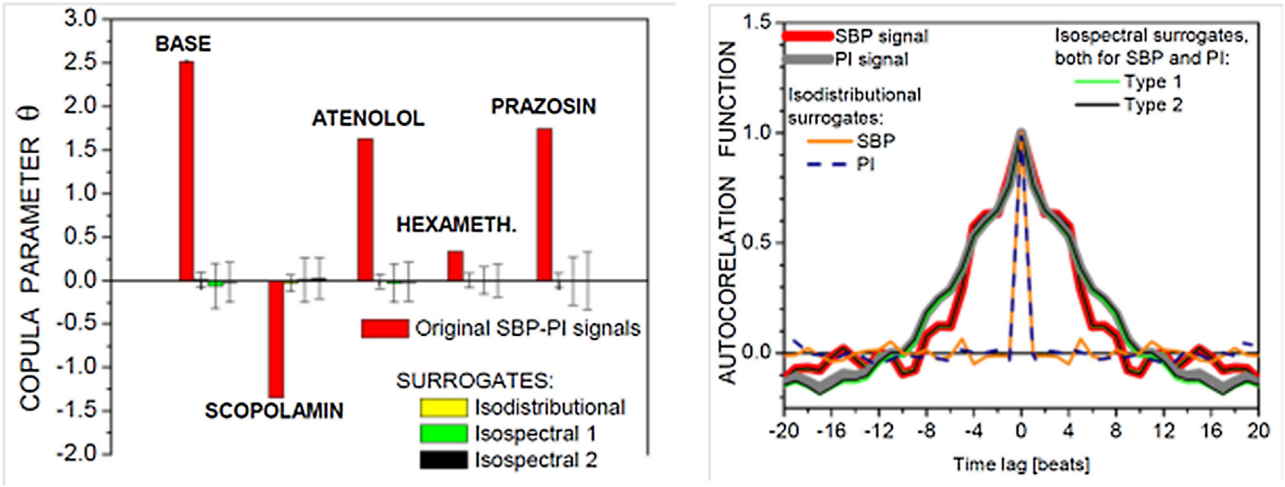

Fig. 14. Copula parameter of original SBP-PI signal pairs and three types of surrogate data (left panel); autocorrelation functions of SBP and PI signals and their surrogates (right panel). Surrogate series are repeated 50 times and the results are presented as mean ± standard deviation.

Table 10
Number of sequences.

	Parallel	Anti-parallel
Baseline	945.2 ± 127.9	216.1 ± 44.0***,
Scopolamine	361.9 ± 28.5++	413.1 ± 23.3++

Results are presented as mean ± s.e.m at DEL = 0. The statistical significance was assessed using repeated measure ANOVA test, Parallel vs. Anti-parallel at level $p < 0.001$ (***) and Baseline vs. Scopolamine at level $p < (0.01)$ (++).

also with the decrease of parallel and the increase of anti-parallel sequences shown in Table 10.

Densities in corner regions of copula plain show the dependency of extreme SBP-PI amplitude levels (tails). The empiric copula densities of SBP-PI signals exhibit weak tail concentration which is correctly modeled by Frank copula.

Surrogate tests with data scrambled both in time and in frequency domains proved that the measured dependency is not a consequence of random occurrences. All five copula methods, as well as Kendall, Spearman, Pearson and Cross-Correlation tests show statistical independence of surrogate SBP and PI time series. These results are also in a perfect accordance with a copula density estimated from isodistributional surrogate data, shown in the bottom rightmost cell of Table 7.

Experimentations with pharmacological denervation and surrogate data clearly indicate that copula recognizes and identifies key neurogenic regulatory mechanism e.i. the BRR behind complex SBP-PI interactions. The baroreceptors located in the aortic arch and carotid sinuses sense discrete changes of BP and adjust PI response on a beat-to-beat basis in order to ensure circulation to all organs. The BRR is seriously affected in cardiovascular diseases, namely neurogenic hypertension and chronic heart failure, and the decrease of BRS has been shown to predict bad clinical outcome (for review see [46]). Hence, further clinical studies are needed to evaluate the possibility of application of copula as an alternative/additional prognostic marker in these conditions.

5. Conclusion

The analysis performed within this paper confirmed an assumption that copulas are useful tool for assessing the static and dynamic linear and non-linear dependency of cardiovascular signals. Possibility of copula to measure level of concordance of SBP and PI and to record behavior of concordance as a function of PI delay in respect of SBP provides an insight into the functioning of the autonomic nervous system. The study showed that the copula method is successful tool for observation of baroreflex in various physiological conditions and, according to that, it could point out on cardiac autonomic dysfunction.

Its particular advantage is a possibility to visualize the dependency structure of the signal and to quantify the dependency changes within the different regions of copula domain. In a case of a healthy organism the symmetric copulas with very weak tail dependencies are the most appropriate for modeling joint distribution function. But, in the cases of arrhythmia or baroreflex impairment, copula should model dependencies within the nonlinear portion of the sigmoidal baroreceptor curve. It could be expected that the best choice of copula type for modeling would be different, asymmetric and with a heavy tails, and that could be subject of further researches. As an additional control for modeling processes, copula generators can create artificial with preserved joint and marginal distributions of the original data.

A bivariate SBP-PI function θ(t,DEL) reflects temporal changes of time lag necessary for signal transmission and integration by the autonomic nervous system and its temporal dependency structure can be observed simultaneously with the recorded subject's behavior.

The drawback of copula is that, as an open loop method, it cannot distinguish the portion of its constitutive feedback and feedforward influences in a way that more complex methods [37] can provide. In the case of multivariate data, multidimensional copula density is not easy to visualize, so a possibility of tomographic presentation would be a topic of future research.

Funding

This research is funded by Grants TR32040 and III41013, Serbian Ministry of Education, Science and Technology development and Telekom Serbia. The funding source had no involvements in study design; in the collection, analysis and interpretation of data; in the writing of the report; and in the decision to submit the article for publication.

Acknowledgments

The last author would like to thank Prof. Laurent Clavier from TELECOM Lille whose presentation at IC1004 COST action inspired this work.

References

[1] E.J. Marey, Physiologie Medicale de la Circulation du Sang, Dalahaye, Paris, 1859, pp. 202–226.
[2] G. Nollo, A. Porta, L. Faes, Causal linear parametric model for baroreflex gain assessment in patients with recent myocardial infarction, Am. J. Physiol. Heart Circ. Physiol. 280 (2001) H1830–H1839.
[3] M. Javorka, Z. Lazarova, I. Tonhajzerova, Z. Turianikova, N. Honzikova, B. Fiser, K. Javorka, M. Baumert, Baroreflex analysis in diabetes mellitus: linear and nonlinear approaches, Med. Biol. Eng. Comput. 49 (2011) 279–288.
[4] G. Parati, M. Di Rienzo, G. Mancia, How to measure baroreflex sensitivity: from the cardiovascular laboratory to daily life, J. Hypertens. 18 (2000) 7–19.
[5] G. Parati, J.P. Saul, P. Castiglioni, Assessing arterial baroreflex control of heart rate: new perspectives, J. Hyppertens. 22 (7) (2004) 1259–1263.
[6] T. Turukalo, N. Japundzic-Zigon, D. Bajić, BP and HRV interactions: spontaneous baroreflex sensitivity assessment, in: Herbert Jelinek, Ahsan Khandoker, David Cornforth (Eds.), ECG Time Series Variability Analysis. Engineering and Medicine, CRC Press, Boca Raton, 2016, p. 9 (Chapter 9).
[7] B.E. Westerhof, J. Gisolf, W.J. Stok, K.H. Wesseling, J.M. Karemaker, Time-domain cross-correlation baroreflex sensitivity: performance on the eurobavar data set, J. Hypertens. 22 (7) (2004) 1371–1380.
[8] D. Laude, J.L. Elghozi, A. Girard, E. Bellard, M. Bouhaddi, P. Castiglioni, C. Cerutti, A. Cividjian, M. Di Rienzo, J.O. Fortrat, B. Janssen, J.M. Karemaker, G. Lefthériotis, G. Parati, P.B. Persson, A. Porta, L. Quintin, J. Regnard, H. Rüdiger, H.M. Stauss, Comparison of various techniques used to estimate spontaneous baroreflex sensitivity (the EUROBAVAR study), Am. J. Physiol. 286 (2004) R226–R231.
[9] M. Di Rienzo, G. Parati, A. Radaelli, P. Castiglioni, Baroreflex contribution to blood pressure and heart rate oscillations: time scales: time-variant characteristics and nonlinearities, Philos. Trans. Royal Soc. A 367 (2009) 1301–1318.
[10] R.W. De Boer, J.M. Karemaker, J. Strackee, Haemodynamic fluctuations and baroreflex sensitivity in humans: a beat-to-beat model, Am. J. Physiol. 253 (1987) H680–H689.
[11] A. Voss, Methods derived from nonlinear dynamics for analysing heart rate variability, Philos. Trans. Royal Soc. A 367 (2009) 277–296.
[12] F. Lombardi, Chaos theory, heart rate variability, and arrhythmic mortality, Circulation 101 (2000) 8–10.
[13] A. Porta, An integrated approach based on uniform quantization for the evaluation of complexity of short-term heart period variability: application to 24 h Holter recordings in healthy and heart failure humans, Chaos 17 (015) (2007) 117.
[14] M. Baumert, M. Javorka, M.M. Kabir, Joint symbolic analyses of heart rate, blood pressure, and respiratory dynamics, J. Electrocardiol. 46 (2013) 569–573.
[15] M. Brennan, M. Palaniswami, P. Kamen, Poincareí plot interpretation using a physiological model of HRV based on a network of oscillators, Am. J. Physiol. Heart Circ. Physiol. 283 (2002) H1873–H1886.
[16] J.M. Tapanainen, P.E. Thomsen, L. Kober, C. Torp-Pedersen, T.H. Makikallio, A.M. Still, K.S. Lindgren, H.V. Huikuri, Fractal analysis of heart rate variability and mortality after an acute myocardial infarction, Am. J. Cardiol. 90 (2002) 347–352.
[17] A. Sklar, Fonctions de repartition a n dimensions et leurs marges, Publ. Inst. Statist. Univ. Paris 8 (1959) 229–231.
[18] J.P. Laurent, J. Gregory, Basket default swaps, CDOs and factor copulas, J. Risk 7 (4) (2005) 103–122.
[19] S. Grimaldi, F. Serinaldi, Asymmetric copula in multivariate flood frequency analysis, Adv. Water Resour. 29 (2006) 1155–1167.
[20] P. Kumar, M.M. Shoukri, Copula based prediction models: an application to an aortic regurgitation study, BMC Med. Res. Methodol. 7 (2007) 21–29.
[21] D. Bajic, T. Loncar-Turukalo, T. Skoric, N. Japundzic-Zigon, Blood pressure and pulse interval coupling: a copula approach, in: Proceedings of 37th Annual International Conference of the IEEE Engineering in Medicine and Biology Society, EMBC 2015, Milan, Italy, August 25–29, 2018, pp. 7696–7699.
[22] H. Joe, Multivariate Models and Dependence Concepts, Chapman and Hall, London, 1997, pp. 12–13.
[23] P. Embrechts, M. Hofert, A note on generalized inverses, Math. Methods Oper. Res. 77 (3) (2013) 423–432.
[24] R.B. Nelsen, An Introduction to Copulas, second edition, Springer Science+Business Media Inc., New York, NY 10013, USA, 2006.
[25] A. Ben, N.E.T. Greville, Generalized Inverses. Theory and Applications, 2nd ed., Springer, New York, 2003.
[26] A.J. McNeil, J. Nešlehová, From archimedean to liouville copulas, J. Multivariate Anal. 101 (8) (2010) 1772–1790.
[27] P. Embrechts, F. Lindskog, A. McNeil, Modelling dependence with copulas and applications to risk management, in: S. Rachev (Ed.), Handbook of Heavy Tailed Distributions in Finance, Elsevier, 2003, pp. 331–385.
[28] R. McNeil, Quantitative Risk Management: Concepts, Techniques and Tools. Princeton Series in Finance, Princeton University Press Princeton, NJ, 2005.
[29] S.S. Santos, D.Y. Takahashi, A. Nakata, A. Fujita, A comparative study of statistical methods used to identify dependencies between gene expression signals, Brief. Bioinform. 15 (6) (2014) 906–918.
[30] C.R. Bhat, N. Eluru, A copula-based approach to accommodate residential self-selection effects in travel behavior modeling, Trans. Res. Part B: Methodol. 43 (7) (2009) 749–765.
[31] C. Constant, D. Laude, I. Murat, J. Elghozi, Pulse rate variability is not a surrogate for heart rate variability, Clin. Sci. 97 (1999) 391–397.
[32] M.P. Tarvainen, P.O. Ranta-Aho, P.A. Karjalainen, An advanced detrending approach with application to HRV analysis, IEEE Trans. Biomed. Eng. 42 (2) (2002) 172–174.
[33] K.J. Hunt, E.S. Fankhauser, Heart rate control during treadmill exercise using input-sensitivity shaping for disturbance rejection of very-low-frequency heart rate variability, Biomed. Signal Process. Control 30 (2016) 31–42.
[34] L. Rüschendorf, Asymptotic distributions of multivariate rank order statistics, Ann. Statist. 4 (1976) 912–923.
[35] F. Durante, J. Fernández-Sánchez, R. Pappadà, Copulas,diagonals,and tail dependence, Fuzzy Sets Syst. 264 (2015) 22–41.
[36] L. Faes, G.D. Pinna, A. Porta, R. Maestri, G. Nollo, Surrogate data analysis for assessing the significance of the transfer function, IEEE Trans. Biomed. Eng. 51 (7) (2004) 1156–1166.
[37] A. Porta, R. Furlan, O. Rimold, M. Pagani, A. Malliani, P. van de Borne, Quantifying the strength of the linear causal coupling in closed loop interacting cardiovascular variability signals, Biol. Cybern. 86 (2002) 241–251.
[38] S. Engelberg, Random Signals and Noise: A Mathematical Introduction, CRC Press, 2007, pp. 130.
[39] A.P. Blaber, Y. Yamamoto, R.L. Hughson, Methodology of spontaneous baroreflex relationship assessed by surrogate data analysis, Am. J. Physiol. 268 (4) (1995) H1682–H1687.
[40] T.G. Coleman, Arterial baroreflex control of heart rate in the conscious rat, Am. J. Physiol. 238 (4) (1980) H515–20.
[41] G.A. Head, R. McCarty, Vagal and sympathetic components of the heart rate range and gain of the baroreceptor-heart rate reflex in conscious rats, J. Auton. Nerv. Syst. 21 (2–3) (1988) 203–213.
[42] T. Tasic, S. Jovanovic, O. Mohamoud, T. Skoric, N. Japundzic-Zigon, D. Bajic, Dependency structures in differentially coded cardiovascular time series, Comput. Math. Methods Med. (2017) 17 (Article ID 2082351).
[43] J. Atkinson, P. Luthi, M. Sonnay, N. Boillat, Effect of acute administration of prazosin on blood pressure, heart rate and plasma renin level in the conscious normotensive rat, Clin. Exp. Pharmacol. Physiol. 13 (7) (1986) 535–541.
[44] K.H. Sanders, I. Jurna, Effects of urapidil, clonidine, prazosin and propranolol on autonomic nerve activity, blood pressure and heart rate in anaesthetized rats and cats, Eur. J. Pharmacol. 110 (2) (1985) 181–190.
[45] P. Castiglioni, M. Di Rienzo, A. Radaelli, Effects of autonomic ganglion blockade on fractal and spectral components of blood pressure and heart rate variability in free-moving rats, Auton. Neurosci. 178 (2013) 44–49.
[46] Japundžić-Žigon, O. Šarenac, M. Lozić, M. Vasić, T. Tasić, D. Bajić, V. Kanjuh, D. Murphy, Sudden death: neurogenic causes, prediction and prevention, Eur. J. Prev. Cardiol. 25 (1) (2018) 29–39.